Support Information

Enhancing organic solar cells lifetime through humidity control using BCF in PM6:Y6 active layers

*Kaike Pacheco, João Paulo Araújo Souza, Marlus Koehler, Eswaran Jayaraman, Daniel Garcia Martos, Vida Engmann, Morten Madsen, Lucimara Stolz Roman**

S1. Experimental Procedures

This study involved three materials: the polymer Poly[(2,6-(4,8-bis(5-(2-ethylhexyl-3-fluoro)thiophen-2-yl)-benzo[1,2-b:4,5-b']dithiophene))−alt−(5,5-(1',3'-di-2-thienyl-5',7'-bis(2-ethylhexyl)benzo[1',2'−c:4',5'−c']dithiophene−4,8-dione)] (PM6), purchased from Brilliant Matters, (2,20-((2Z,20Z)-((12,13-bis(2-ethylhexyl)-3,9-diundecyl-12,13-dihydro-[1,2,5]thiadiazolo-[3,4-e]thieno[2”,3” : 4',5']thieno[2”,3” : 4,5']pyrrolo[3,2-g]-thieno[2”,3” : 4,5']thieno[3,2−b]indole−2,10−diyl)bis(methanylylidene))bis(5,6−difluoro−3−oxo−2,3−dihydro−1H−indene−2,1−diylidene))dimalononitrile (Y6) [purchase information], and Tris(pentafluorophenyl)borane (BCF) also purchased from Brilliant Matters.

The glass and ITO substrates obtained from Kintec were subjected to a thorough cleaning process. Initially, each substrate was sonicated for 15 minutes in Extran detergent using ultrasound. Subsequently, the substrates underwent a meticulous rinse with deionized water while being sonicated for an additional 15 minutes. This same sonication process was then repeated using acetone, followed by a similar treatment with isopropyl alcohol (IPA). Upon completing these cleaning steps, the films were meticulously dried by gently blowing them dry with N_2.

For film preparation, blend solutions were meticulously prepared with a PM6:Y6 ratio of 1:1.2 for the pure devices, and a PM6:Y6 ratio of 1:1.2 with the incorporation of 2% mass of BCF material. The total concentration used in these solutions was 17 mg/ml, and they were carefully diluted in a mixture of chlorobenzene and chloronaphthalene in a ratio of 1:0.5%. A detailed investigation regarding the quantity of BCF needed to influence the device's lifespan without compromising the conversion efficiency was conducted and can be found in the supplementary information file. It's important to note that the same solution was uniformly applied to all devices and films involved in this experiment.

The devices employed in both the power conversion efficiency (PCE) and lifetime studies adhered to the configuration outlined in Table S1. These films were deposited onto the pre-existing ITO layer, which had previously been coated onto Kintec substrates [1].

Table S1: Architectures used for the three types of devices studied.

Type	Architecture
Regular	ITO/ZnO/ActiveLayer/MoO_3/Ag
Electrons Only	ITO/ZnO/ActiveLayer/ZnO/Ag
Hole Only	ITO/PEDOT:PSS/ActiveLayer/MoO3/Ag

With the exception of MoO3 and silver, which were deposited through evaporation with thicknesses of 10 nm and 100 nm, respectively, all other materials underwent a spin-coating process. Specifically, ZnO was spin-coated at 3000 rpm for a duration of 60 seconds, and this procedure was applied to both ZnO films. The ZnO layer on ITO underwent further baking at 130°C for a period of 10 minutes. The active layer was spin-coated at 3500 rpm for 30 seconds, followed by baking at 100°C for 10 minutes. PEDOT:PSS was spin-coated at 4000 rpm for 40 seconds and subsequently baked at 130°C for 20 minutes.

Device fabrication took place within a glovebox environment filled with nitrogen (N_2), except for certain devices used in charge mobility measurements. These particular devices were fabricated outside the glovebox to investigate electrical parameters in the presence of BCF interacting with water in fresh devices.

All devices underwent J-V measurements using an Enlitech solar simulator. The regular devices were subjected to continuous 1 sun illumination in a PV infinity solar simulator equipped with UV protection, adhering to the ISOS-L-1 standard for light immersion [2]. J-V measurements were recorded at 45-minute intervals. Charge mobility devices followed a similar degradation process but were subsequently returned to an inert environment for post-degradation J-V measurements performed in darkness. AFM and EQE measurements were conducted following the same procedure.

UV-VIS measurements were conducted using a Shimadzu spectrometer. Films were subjected to degradation within the same environment as the devices and were measured on an hourly basis. FTIR measurements were carried out on films deposited onto CaF2 (Crystran) substrates using a Shimasdy IRAffinity-1S spectrometer.

S2. Performance parameters of fresh devices.

Table S2. Performance parameters of fresh devices.

Active Layer	BCF concentration	Voc (V)	Jsc (mA/cm^2)	FF	PCE (%)
PM6:Y6	-	0.81 ±0.01	25.33 ±0.30	0.63±0.01	14.32±0.16
PM6:Y6:BCF	2	0.81 ±0.01	26.10 ±0.36	0.63±0.01	14.52±0.13

S3. Molecular dynamics simulations Page 2

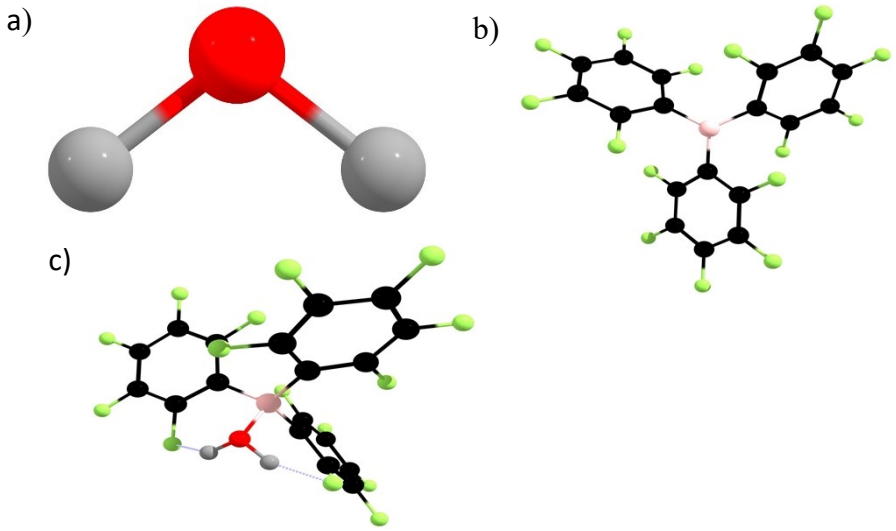

Figure S1: (a) water molecule (b) BCF and (c) Interaction of the water molecule with the BCF.

S4. Calculation details

We apply Density Functional Theory (DFT) to study the main properties and interactions of PM6, BCF and water. All DFT calculations were performed using the Gaussian 16.1 package. The optimization to obtain the lower energy geometry were performed using the ωB97XD,2 functional (which is capable of capturing short and long range interactions) together with the 6-31G(d,p) basis set.3,4 To compute the Gibbs free energy, we analyze the vibrational modes of the PM6, BCF and water molecules alone. Subsequently, we performed the same analysis with the interaction of PM6 and BCF and then PM6, BCF, and water considering three regions 1, 2, and 3 of interaction highlighted in Figure 4. The vibrational analysis was calculated using DFT/ ωB97XD/6-31G(d,p) level of theory.

It is inferred that the reaction of BCF with water generates protons, which subsequently associate with PM6 through bonding to the sulfur atom. Yu Cui and co-authors [3] theoretically investigated the interaction between BCF(OH2) and the Y6 molecule in two specific configurations: (i) the BCF(OH2) complex next to the acceptor's end of Y6 and (ii) the complex interacting with central group of Y6. The calculation indicated that there is a twist in the structure of Y6 due to the proximity with the BCF(OH2) adduct. This result suggests that there is indeed an interaction between the two systems, but it was not observed any variations in the length of the H-O bonds of the water molecule. The absence of changes in the H-O bond of the was indicates that there is not a strong direct interaction involving a proton transfer to the sulfur atoms of the Y6 molecule. In addition, the authors[1] found that that the variation of the Gibbs free energy upon interaction of the BCF(OH2) adduct with the Y6 is lower compared to the variation

1 - This interaction was calculated by some of the authors to the article [3]. However, the value of free energy variation (-28.7334, for the interaction of BCF(H20) with the edge of Y6 molecule, respectively) was not explicitly mentioned in the text since it originated from an inquiry during the review process.

calculated for the BCF(OH2)/PTQ10 system. All those findings suggest that, despite the presence of sulfur

1 - This interaction was calculated by some of the authors to the article [3]. However, the value of free energy variation (-28.7334, for the interaction of BCF(H20) with the edge of Y6 molecule, respectively) was not explicitly mentioned in the text since it originated from an inquiry during the review process.

atoms in Y6, the interaction between the BCF-H2O complex and PM6 is more intense. The reason behind this behavior be associated to differences in the accessibility or reactivity of the sulfur sites in Y6 compared to PM6. In conclusion, this research demonstrates that the addition of BCF offers intrinsic protection to OSCs by a predominant interaction with the polymer, leading to significant advances in their durability.

S5. Molecular orbitals

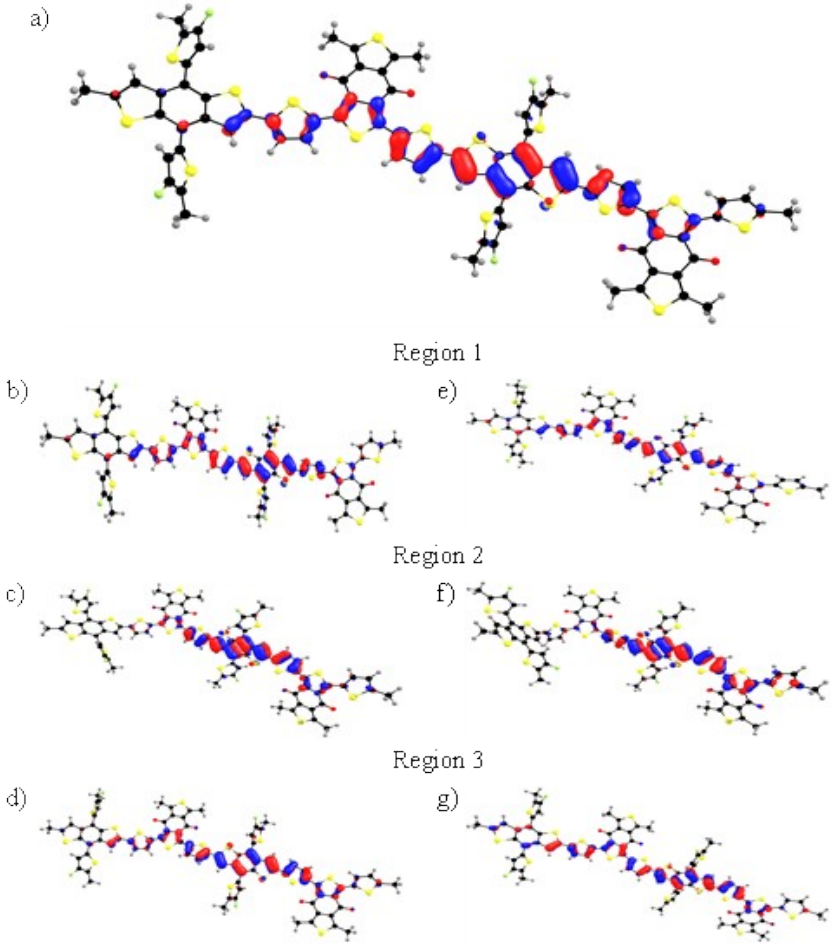

Figure S2: Molecular orbitals of an isolated PM6 oligome are depicted in figure (a). Figures (b), (c) and (d) illustrate the molecular orbitals of the polymer post-interaction with BCF in regions 1, 2, and 3 respectively. Similarly, figures (e), (f) and (g) represent the molecular orbitals of PM6 post interaction with BCF and water in regions 1, 2, and 3 respectively**.**

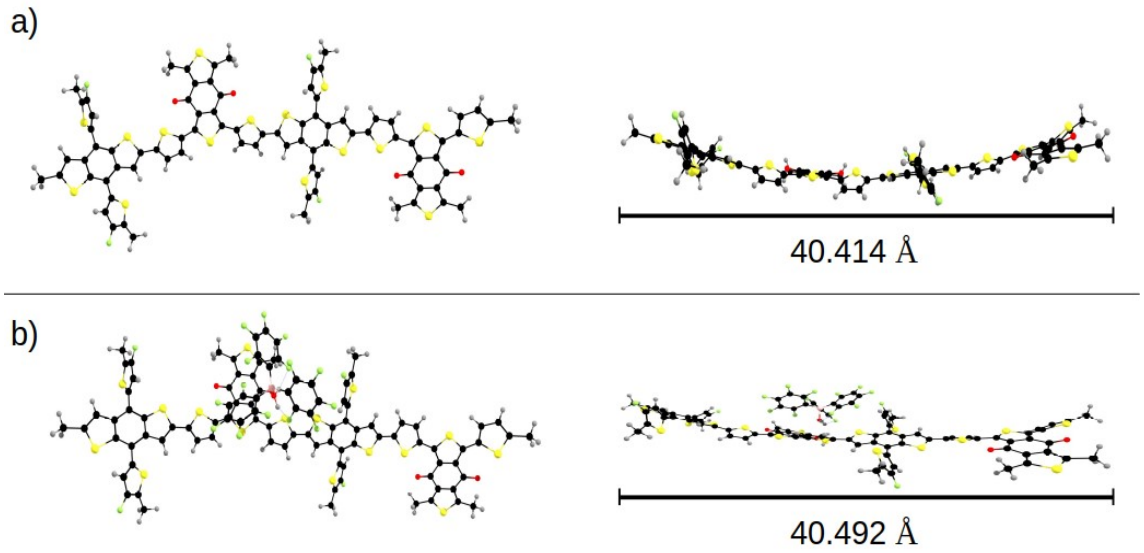

Figure S3: Resulting optimized chemical structure of an isolated PM6 oligomer (b) and the PM6 oligomer in the presence of the BCF/H_2O system.

Table S3: Analysis of the variation in Gibbs free energy.

Molecule	ΔG (eV)	ΔG (eV)	ΔG (eV)
BCF	2.5876	2.5876	2.5876
H2O	0.0970	-	0.0970
PM6	-	24.8038	24.8038
Sum of Gibbs Energy (SGE)	2.6846	27.3914	27.4884
Trimers	ΔG (eV)	$\Delta G_{SGE,\Delta G}$ [SGE-ΔG] (eV)	$\Delta G_{SGE,\Delta G}$ [SGE-ΔG] (Kcal/mol)
PM6/BCF/H2O	28.7958	-1.3074	-30.1493

S6. Space charge Limited current

Charge mobility devices underwent the same degradation process as photovoltaic devices but were returned to the inert environment for post-degradation J-V measurements in the dark. Additionally, the devices were fabricated with exposure to a non-inert environment (outside the glovebox) to induce the interaction of BCF with water molecules and examine how the activated BCF influences the charge mobility of the material. They present the architecture as shown in Figure1b for electrons only, ITO/ZnO/Active Layer/ZnO/Ag and

Figure1c for holes only, ITO/PEDOT:PSS/Active Layer/MoO3/Ag. The analysis of charge mobility was conducted using two approaches. Firstly, the devices were measured immediately after fabrication in an inert environment, representing the initial state (first measurement). Subsequently, the same devices were subjected to the ISOS-L-1 light soaking degradation system for a period of 7 hours and the measurements were repeated to assess the changes in charge mobility post-degradation. The measured values for hole mobility were μh=3.48*10−4[cm2V −1S−1] for the pure device and μh = 3.96*10−4[cm2V −1S−1] for the doped device. These experiments demonstrate an improvement in hole mobility when BCF behaves as a Brønsted acid.

Table S4. Charge mobility comparison - $10^{-4}[cm^2V^{-1}S^{-1}]$.

a) Hole Mobility (m_h)

AL	Fresh	Aged
Pure	3.4	2.6
Doped	3.3	3.0

b) Electron Mobility (m_e)

AL	Fresh	Aged
Pure	3.49	2.65
Doped	3.08	2.25

The comprehensive analysis of charge mobility presented in Table S2, combined with the optical analysis depicted in Figure 4, provides valuable insights into the underlying factors influencing the observed behavior of the PCE curve illustrated in Figure 7 by establishing these connections, our findings contribute to a more comprehensive understanding of the factors influencing the overall performance of organic photovoltaic devices.

From the release of H+ in the active layer, due to the BCF + H2O interaction, strongly suggested by this work, the interaction of this atom with PM6 not only slows down the degradation but would also have the potential to improve the properties of electrical connections, as shown in Figure 2b. This work explores a unique approach with BCF in OSC's, demonstrating that BCF not only delays degradation by capturing water molecules but also improves certain electrical parameters of the active layer, compensating for degradation-induced losses.

S7. FTIR complementation spectra

To further support the findings presented in Figure 6, Figure S4 illustrates the FTIR spectra of PM6 alone, both with and without BCF. This comparison highlights the interaction of BCF with the PM6 molecule in the absence of Y6, providing additional insights into the molecular interactions at play.

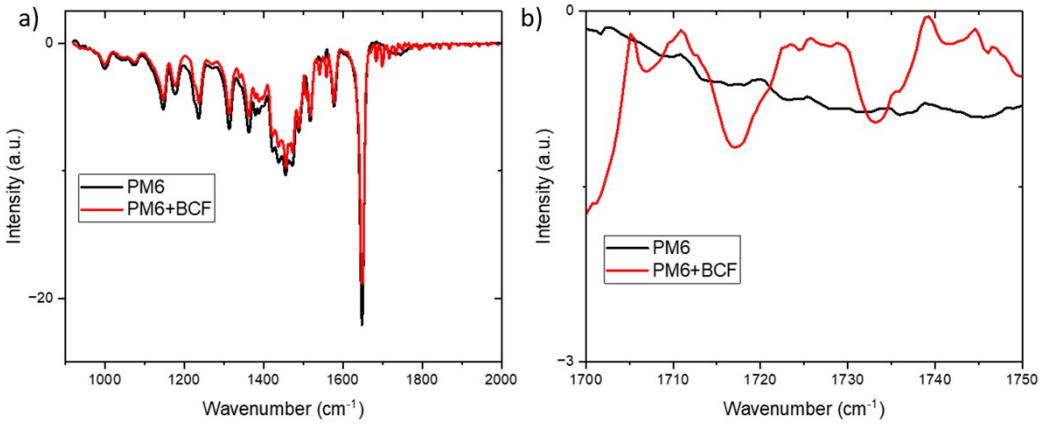

Figure S4: FTIR spectroscopy of a) PM6 and b) PM6+BCF fresh.

References

[1] M. Ahmad et al., “Uncovering the Electronic State Interplay at Metal Oxide Electron Transport Layer/Nonfullerene Acceptor Interfaces in Stable Organic Photovoltaic Devices,” ACS Appl Mater Interfaces, 2023, doi: 10.1021/acsami.3c11103.

[2] M. O. Reese, S. A. Gevorgyan, M. Jørgensen, E. Bundgaard, S. R. Kurtz, D. S. Ginley, D. C. Olson, M. T. Lloyd, P. Morvillo, E. A. Katz, et al., Consensus stability testing protocols for organic photovoltaic materials and devices, Solar Energy Materials and Solar Cells 95 (5) (2011) 1253–1267.

[3] M. J. Frisch, G. W. Trucks, H. B. Schlegel, G. E. Scuseria, M. A. Robb, J. R. Cheeseman, G. Scalmani, V. Barone, B. Mennucci, G. A. Petersson, et al. Gaussian 16, Revision C.01. Gaussian, Inc., Wallingford CT, 2016.

[4] J.-D. Chai, M. Head-Gordon. Long-Range Corrected Hybrid Density Functionals with Damped Atom–Atom Dispersion Corrections. Phys. Chem. Chem. Phys., 2008, 10 (44), 6615–6620.

[5] W. Zhao, D. Qian, S. Zhang, S. Li, O. Inganäs, F. Gao, J. Hou. Fullerene-Free Polymer Solar Cells with over 11% Efficiency and Excellent Thermal Stability. Adv. Mater., 2016, 4734–4739.

[6] Z. Zheng, J.-L. Brédas, V. Coropceanu. Description of the Charge Transfer States at the Pentacene/C60 Interface: Combining Range-Separated Hybrid Functionals with the Polarizable Continuum Model. J. Phys. Chem. Lett., 2016, 7 (13), 2616–2621.